



## Removal of methylene blue dye from synthetic aqueous solutions using novel phosphonate cellulose acetate membranes: adsorption kinetic, equilibrium, and thermodynamic studies

Randa E. Khalifa<sup>a</sup>, Ahmed M. Omer<sup>a</sup>, Tamer M. Tamer<sup>a</sup>, Waheed M. Salem<sup>b</sup>,  
Mohamed S. Mohy Eldin<sup>a,\*</sup>

<sup>a</sup>Polymer Materials Research Department, Advanced Technology and New Materials Research Institute (ATNMRI), City of Scientific Research and Technological Applications (SRTA-City), New Borg El-Arab City 21934, Alexandria, Egypt, emails: mmohyeldin@srtacity.sci.eg (M.S. Mohy Eldin), randaghonim@yahoo.com (R.E. Khalifa), ahmedomer\_81@yahoo.com (A.M. Omer), ttamer85@yahoo.com (T.M. Tamer)

<sup>b</sup>Chemistry Department, Faculty of Science, Damanshour University, Damanshour, Egypt, email: waheedsalem1979@yahoo.com

Received 21 April 2018; Accepted 18 October 2018

### ABSTRACT

In this study, novel phosphonated cellulose acetate (PCA) membranes were used for adsorptive removal of cationic methylene blue (MB) dye under batch conditions and different preliminary concentrations of the pollutant and pH values at 25°C. The chemical structure of PCA membranes was established by Fourier transform infrared spectrophotometric analysis. Adsorption kinetics, isotherms, and thermodynamics were examined. The analysis of three kinetic models specifically pseudo-1st-order model, pseudo-2nd-order model, and Elovich model was performed. The rate of MB adsorption was found to accompany pseudo-2nd-order model. Adsorption data of MB have also been used to test various adsorption diffusion models. The diffusion rate modeling of Dumwald-Wagner and the intraparticle diffusion model have been used to determine the diffusion rate and the rate-controlling step. Boyd expression was also used to give the accurate indications. Sorption equilibrium of MB by PCA membranes was also quantitatively evaluated by isotherm models of Langmuir, Freundlich, Dubinin-Radushkevich, and Temkin. Adsorption behaviour followed the Langmuir adsorption isotherms ( $q_{\max} = 10 \text{ mg/g}$ ). Finally, the negative  $\Delta G^\circ$  values designated that the MB adsorption onto sorbent membranes was viable and spontaneous, while the positive  $\Delta H^\circ$  value depicted that MB removal is endothermic.

*Keywords:* Cellulose acetate; Methylene blue; Kinetics; Isotherms; Thermodynamics

### 1. Introduction

Up to date, water contamination is one of the worst of all environmental problems through the continuous direct discharge of hazardous and toxic chemical effluents to the surroundings [1]. Dye-contaminated wastewater contains coloured compounds from residues of dyes and many

chemical spices. Basic, acid, direct, and reactive dyes are soluble in water, while oxidised dyes and dispersed pigments are insoluble. Synthetic dye pollutants from industrial activities, for example, textile, food industries, leather, plastics, cosmetics, pharmaceuticals, dye synthesis, silk painting [2], and printing, are carcinogenic and highly toxic. It caused more and more interest as over 10,000 categories of dyes have been utilised in the industry [3]. Most dyes' attitude poses a significant threat to health, the well-being of

\* Corresponding author.

millions of people, microbial population, marine lives, and environments [4], and global ecosystems. Furthermore, the coloured water retarded the sunlight, hindered the activity of photosynthetic process of the aquatic plants, impedes the growth of biota, and also has a propensity to chelate metal ions which produce micro-toxicity to fish and other organisms [5]. Among the different synthetic dyes, methylene blue (MB) is extensively a typical compound in adsorption studies. The existence of 14 delocalized electrons in the planar structure of the dye efficiently involves in stacking interactions. Consequently, MB can form dimers and privileged aggregate levels in aqueous solutions even at micromolar analytical concentrations [6]. The association of stacking interaction and Columbic forces governs the excellent adsorptive characteristics of this type of dyes [7]. Therefore, MB is quickly attracted to hydrophilic surfaces carrying net negative charges. Traditional treatment approaches such as zonation, biodegradation, and oxidation [8] are not successful in dye removal due to the complex aromatic structures, which mark them much stable. Alternatively, a variability of conventional treatment methods including physical and chemical techniques is intended for dye exclusion from industrial wastewater. Flocculation and coagulation, reverse osmosis, ion exchange, activated sludge, adsorption by activated carbon, electrochemical methods, etc. are moreover expensive or even ineffective [9] and always show many disadvantages. To our delight, adsorption technology was economically useful, cheap, simple, and efficient, and the easy operation did not produce contaminated by-products. Numerous resources have dedicated into the adsorption researches, such as zeolite, wood [10], silica, coir pith, peat [11], sawdust [12], fly ash [13], and almond shells. Another point worth mentioning is that the processing cost may be minimised by the low-cost adsorbent materials, like waste material, biosorbent, sludge, and clay including bentonite, kaolinite, talc, montmorillonite, and agricultural by-products. MB is readily adsorbed onto an extensive range of adsorbents from industrialised wastewater [14] to innovative materials [15] including modified minerals [16]. Recently, researchers paid massive attention to natural occurring polymers as chitosan [17], alginate [18], and cellulose [19] because of their compatibility with any biological systems, biodegradability, and availability and on their excellent adsorptive properties. However, the hydrophilic natural surroundings of these biopolymers accompanied by the abundance of the reactive -OH groups are responsible for the mechanical unpredictability of these polymers which bound their applicability. Noteworthy efforts were rendered to improve unconventional adsorbents through chemical modification, but, owing to low mechanical strength, these developed adsorbents were commercially unsuccessful. So, significant determinations have tended to enhance the performance of such polymers by calendaring an ion exchange material into the plastic film or in polymeric solution such as alumina, zirconia, titania, silver, and silica particles [20,21]. Recently, researchers have investigated the outcome of additives as nanoparticles, inorganic fillers, various surfactants [22,23], and variant functional groups like carboxylic (COO-), sulfonic (SO<sub>3</sub>-), and phosphonic (PO<sub>3</sub>-) [24,25] by chemical modification. Moreover, synthesis of polymer blend [26], selection of different polymeric matrices [27], and variation of cross-linker have been investigated. In addition to surface modification by plasma coating technique [28], use of various

solvents allotment of uniform functional groups distribution over the modified polymer adsorbents. All these parameters are simple means to realise higher ionic exchange material. Recent work has explored applying adsorption/ion exchange to water polluted with an extensive range of sensitive dyes [29–31]. However, most commercial ion exchangers are present in the formula of the porous structure; thus, their packed bed operation for flow process commonly has certain restrictions such as sluggish pore dispersion, high-pressure drop, etc. An encouraging alternate for eliminating these problems is the ion exchange membrane. The membrane system could not only overcome the mass transference confines for packed beds but also exhibit the advantages of simpler design and easier scale-up. Therefore, the ion exchange film should be a respectable choice for dye adsorption, and the interrelated performance should be intensively estimated. Nevertheless, the prospective application of macroporous ion exchange membranes to dye withdrawal from wastewater has been ignored. Cellulose is considered the utmost plentiful natural polymer established in normal fibres and plants. Etherification of cellulose produces many derivatives of water-soluble cellulose such as hydroxy ethyl cellulose, hydroxy propyl cellulose, ethyl cellulose, or sodium carboxymethyl cellulose. In this study, a cellulosic adsorbent membrane was fabricated by chemical activation of cellulose acetate (CA) using epichlorohydrin (ECH) followed by the introduction of orthophosphoric acid (OPA) for the removal of MB from aqueous solution. Batch adsorption was conducted at several initial MB concentrations and solution pH at 25°C. Adsorption kinetics and equilibrium isotherms for the exclusion of MB on phosphonated cellulose acetate (PCA) membranes were evaluated to demonstrate the adsorption type of dye removal. Also thermodynamics were also determined to distinguish the nature of adsorption process.

## 2. Experimental

### 2.1. Materials

CA (degree of acetylation 40%) and ECH (purity 99.5%) were supplied from Sigma-Aldrich Chemie GmbH (USA). Ortho phosphoric acid (purity 85% extra pure), acetone (purity 90%), hydrochloric acid (purity 95%–97%), and MB were acquired from Sigma-Aldrich Chemicals Ltd. (Germany). Sodium hydroxide was supplied by El-Nasr Company for Chemicals (Egypt).

### 2.2. Methods

#### 2.2.1. Membrane preparation

The PCA solution was synthesised as mentioned in our previous work [32]. Briefly, CA was dissolved in acetone under regular stirring. Then ECH (1:3, molar ratio of CA:ECH) was added gradually. The activated solution was agitated at 25°C for 5 h, and the solution pH was adjusted using sodium hydroxide solution. Then, the activated cellulose acetate solution was retained at a water steam bath at 55°C for 9 h and pH 8 with constant shaking. Subsequently, the obtained viscous and transparent activated solution reacted with 1.5M OPA aqueous solution. The phosphorisation process was carried out in a water bath at 35°C for 8 h. The casting solutions termed PCA1.5 solution were obtained and allowed to

cool at 25°C (Fig. 1). The casting solution was then spread over a smooth glass plate, and the film was exposed to air for 3 min at 25°C, by which the macroporous structure has been formed for PCA1.5 membranes [33]. Then, the film with glass plate was immersed in a deionised water bath until the membrane turned white and separated from the glass plate. The prepared films were finally rinsed with deionised H<sub>2</sub>O and then dried for another 24 h at 25°C.

### 2.2.2. Adsorption studies

All batch adsorption experimentations were conducted using a pre-weighed sample of the developed membranes (0.2 g, 1 cm × 1 cm) in addition to a known volume of dye solution (50 mL). Specific weight of MB solubilised in distilled water was used to prepare the required dye solution concentration. Then, the mix was stirred by constant shaking at a rate of 120 rpm. Subsequently, the remaining dye concentration in the solution was measured via UV-visible spectrophotometer (Amersham Pharmacia Biotech, UK Ltd.) at 668 nm wavelengths. The MB level used in this investigation is 10 mg/L for kinetics and a range of 10–100 mg/L for isotherms at 298 K and at different time intervals. Percent removal of the dye expresses the adsorption efficiency. The adsorbed extent ( $q$ ) of the MB at time ( $t$ ) is evaluated by the following equations [34]:

$$\% \text{Removal} = \frac{C_0 - C_t}{C_0} \times 100 \quad (1)$$

$$q = \frac{(C_0 - C_t)}{W} \times V \quad (2)$$

where  $q$ , the adsorbed quantity of dye/gram adsorbent (mg/g);  $C_0$  the primary dye concentration (ppm);  $C_t$  the dye strength at time  $t$  (ppm);  $V$ , the volume of the MB solution (L); and  $W$ , the adsorbent weight (g).

### 2.2.3. Adsorption kinetics

The performance and eventual cost of adsorption system are substantially dependent on the efficiency of technical design and effectiveness of sorption operation, which often involves a synergetic of the uptake kinetics or the time dependency of concentration dispersal of the solute in both bulk and solid phase [35]. The adsorption progression involves the mass transfer of a solute from the fluid phase to the adsorbent surface [36]. A kinetic reading of adsorption provides consequences for the adsorption mechanism [37]. Also, this dynamic study defines the solute uptake rate that manages the residence time of adsorbate uptake at the solid surface interface [38]. Numerous kinetic models were adapted to predict the controlling adsorption mechanisms (such as chemical reaction, diffusion control, and mass transfer), and the best-fit model will be selected by the linear regression correlation coefficient and  $R^2$  values.

#### 2.2.3.1. The pseudo-1st-order model

The pseudo-1st-order model has correlated the adsorption rate with the adsorption capacity. This model rate equation is stated as follows [39]:

$$\frac{dq_t}{dt} = k_1 (q_e - q_t) \quad (3)$$

By integrating Eq. (3), using the first situation  $q_t = 0$  when  $t = 0$ , the following equation will be obtained:

$$\ln(q_e - q_t) = \ln q_e - k_1 t \quad (4)$$

where  $q_e$  and  $q_t$  are the adsorbed amounts of MB at steady state (mg/g) and  $k_1$  is the rate constant of pseudo-1st-order adsorption (/min). Since  $q_t$  reaches a plateau  $q_e$  at equilibrium,  $q_t$  values smaller than the  $0.9 q_e$  were used for analysis.

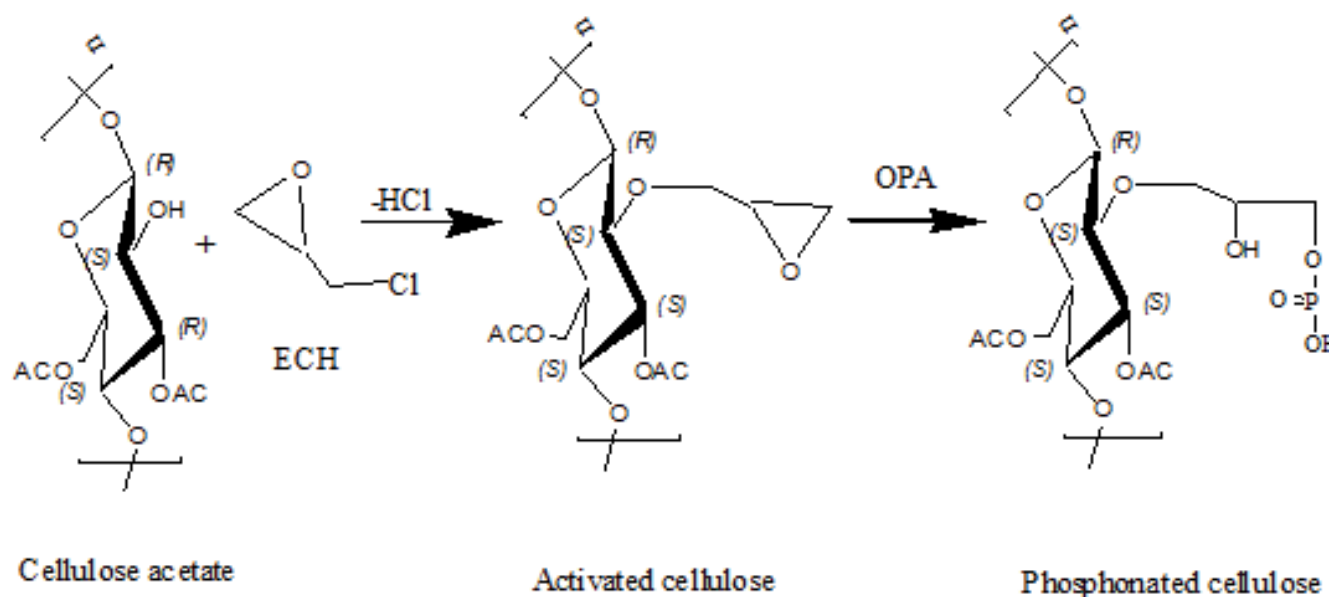


Fig. 1. A mechanistic pathway for the synthesis of PCA solution.

### 2.2.3.2. The pseudo-2nd-order model

The pseudo-2nd-order kinetic rate equation (Ho's model) is signified as follows [40]:

$$\frac{dq_t}{dt} = k_2(q_e - q_t)^2 \quad (5)$$

where  $k_2$  is the pseudo-2nd-order rate constant (g/mol min). Resetting the variables in Eq. (5) gives:

$$\frac{dq_t}{(q_e - q_t)^2} = k_2 dt \quad (6)$$

Taking into consideration the boundary status from  $t = 0$  to  $t = t$  and  $q_t = 0$  to  $q_t = q_t$ , the integrated form of Eq. (6) be ordered to obtain the resulting equation:

$$\frac{1}{q_e - q_t} = \frac{1}{q_e} + k_2 t \quad (7)$$

Eq. (7) can be reconstructed to get a linear form:

$$\frac{t}{q_t} = \frac{1}{k_2 q_e^2} + \frac{t}{q_e} \quad (8)$$

The initial adsorption rate  $h$  (mol/g min) is expressed as:

$$h = k_2 q_e^2 \quad (9)$$

A lined relationship will be obtained from the plan of  $(t/q_t)$  vs  $t$  from which  $k_2$  and  $q_e$  can be ascertained. The half-adsorption time,  $t^{0.5}$ , is designated as the time expected for the adsorption to hold half as much MB as its equilibrium value. Accordingly, this  $t^{0.5}$  value is a measurable tool of the sorption rate:

$$t^{0.5} = \frac{1}{k_2 q_e} \quad (10)$$

### 2.2.3.3. Elovich equation

In reactions concerning chemisorption of adsorbate molecules on the solid surface deprived of products released, the rate declines with time because of an improved solid surface coverage. Elovich equation is a helpful model for explaining such an activated process [41]:

$$\frac{dq_t}{dt} = \alpha \exp(-\beta q_t) \quad (11)$$

where  $\alpha$  is the original adsorption rate (mol/g min) and  $\beta$  is relevant to surface coverage extent and activation energy for chemisorption (g/mol). The latter equation explains the linear pattern of the Elovich model:

$$q_t = \beta \ln(\alpha\beta) + \beta \ln t \quad (12)$$

The testing of empirical data for correspondence with the Elovich equalisation is conducted via plotting  $q_t$  vs.  $\ln t$ . The Elovich parameter  $\beta$  and the primary rate  $\alpha$  are received from both inclination and intercept of the line. The applicability of the Elovich equation suggests that chemisorption (chemical reaction) mechanism is likely to rate control in the current processes [42].

### 2.2.4. Rate-limiting kinetic models

The adsorption operation can recognise as a sequence of three progressive steps; namely, (a) film diffusion, (b) particle diffusion, and finally (c) adsorption of the adsorbate molecule on the internal surface of the adsorbent. In contrast, the rate-determining stage is highly dependent on the velocity of each step. Then, this period is highly dependent on the velocity of each step. Conversely, if the velocity of two is exceeding that of level one, particle diffusion and vice versa will control the adsorption speed. However, when the exterior transport is equal to an interior carrier, a boundary of liquid film will form around the adsorbent particles; in this occasion, the dispersion of adsorbate follows the appropriate concentration gradient. Three consolidated kinetic models can be practical to solve this common problem.

#### 2.2.4.1. The Weber–Morris intraparticle diffusion

Rate constant ( $k_p$ ) provided by the next equation [43]:

$$q_t = k_p t^{0.5} + C \quad (13)$$

where  $k_p$  is the intraparticle diffusion rate constant (mol/g min<sup>1/2</sup>). Such plots might exhibit a multilinearity [44], symbolising that two or further rounds take place. The first is the active division assigned to the distribution of adsorbate inside the liquid phase to the outer adsorbent surface or the borderline layer diffusion of sorbent molecules or ions. The secondary portion describes the successive adsorption step, where intraparticle dissemination is rate limiting. The third portion is credited to the last equilibrium step wherever intraparticle dispersal begins to break down due to insufficient adsorbate levels in the solution. The solute uptake rate might be bounded by many factors including the size of adsorbate ions or molecules, the strength of the dye and its attraction to the adsorbent, the diffusion coefficient of dye in the bulk side, the pore extent configuration of the sorbent material, and the mixing degree. Additionally, the estimation of  $C$  gives a good impression about the obstacle layer thickness, i.e., the boundary layer influence is more significant at a higher value of  $C$ , where the intraparticle diffusion governs the process if  $C = 0$ .

#### 2.2.4.2. Dumwald-Wagner model

The diffusion rate equation of Dumwald-Wagner (D-W) model [45] inside the adsorbent particle is expressed by

$$\log(1 - F^2) = \frac{K}{2.303} \times t \quad (14)$$

where  $K$  is the diffusion rate constant (1/min) and  $F$  is the adsorption ratio ( $F = q_t/q_e$ ). The plot of  $\log(1 - F^2)$  vs

$t$  demonstrates the possibility of using this, consistent with the  $R^2$  values (correlation coefficient).

### 2.2.4.3. Boyd model

Boyd et al. established the single resistance system model and examined that the adjacent boundary layers to the sorbent particles are the major resistance towards gas diffusion which switches the adsorption speed. This model may be indicated by [46]

$$F = 1 - \frac{6}{\pi^2} \sum_{n=1}^{\infty} \frac{1}{n^2} \exp(-n^2 Bt) \quad (15)$$

where  $F$  is the fractional adsorption capacity constant at any time and can be estimated as follows  $F = q_t/q_e$ .  $Bt$  (rate coefficient) is a parameter for the particle diameter ( $2r$ ), adequate diffusion coefficient (Deff), and also a function of  $F$ .

$$Bt = \left( \sqrt{\pi} - \sqrt{\pi - \left( \frac{\pi^2 F}{3} \right)} \right)^2 \quad \text{For } F < 0.85 \quad (16)$$

$$\text{And } Bt = -0.498 - \ln(1 - F) \quad \text{For } F > 0.85 \quad (17)$$

$$Bt = -0.4978n - \ln(1 - F) \quad (18)$$

Plotting  $Bt$  vs.  $t$ , gives a straight line or a nonlinear curve not intersecting crossing the origin, illustrates that the film diffusion will play a significant role in handling the adsorption manner.

### 2.2.5. Adsorption isotherms

The adsorption equilibria are one of the standard fundamental approaches used to predict the adsorption trend. Isotherms are also beneficial for explaining adsorption capacity that facilitates evaluation of the practicability of this process for a particular application. Also, it is helpful in selecting the most suitable adsorbent, as well as a preliminary decision about the required adsorbent dosage [47]. At this point, it can supply more knowledge about the sorbent surface properties, the design of the system and the relationship between the mass of solute adsorbed/unit mass of the solid adsorbent and liquid phase dye concentration at a definite temperature. Additionally, adsorption equilibrium gives a reasonable implication of the way in which the adsorbed dye molecules allocate between the liquid and solid medium at equilibrium.

Furthermore, the adsorption equilibrium is a dynamic impression achieved as the rate of MB adsorption is equal to the adsorption rate. Hence, the dye adsorption onto the PCA1.5 membranes was determined as a function of the equilibrium concentration of the MB aqueous solution. The experimental data were en suite directly to the standard nonlinear two-parameter Langmuir [48] and Freundlich [49] models and the three-parameter models [50] Dubinin-Radushkevich (D-R) [51] and Temkin [52].

#### 2.2.5.1. Langmuir isotherm model

This isotherm is the utmost valid model for the removal of several pollutants from an aqueous solution by adsorption. The assumption is based on the fact that sorbent surface is structurally homogeneous, and the adsorption sites can only fill by one dye molecule to form monolayer adsorption on a consistent surface with a limited number of energetically equivalent and identical active sites. Once saturation was reached, no more adsorption can transpire, and the highest adsorption capacity will gain. The following linear equation can give the saturated monolayer isotherm:

$$\frac{C_e}{q_e} = \frac{1}{q_{\max} K_L} + \frac{C_e}{q_{\max}} \quad (19)$$

where  $C_e$  is the equilibrium MB concentration (mg/L),  $q_e$  is the adsorbed amount of dye at equilibrium (mg/g),  $q_{\max}$  is the supreme monolayer coverage capacity (mg/g), and  $K_L$  is the Langmuir equilibrium constant (L/g) which is related directly to the surface free energy.  $K_L$  and  $q_{\max}$  constants were obtained from the  $C_e/q_e$  vs.  $C_e$  plot.

Furthermore, to divine the extent to how the adsorption operation is satisfactory [48], the isotherm shape has been considered. The fundamental characteristic of the Langmuir model can be revealed using a dimensionless constant 'RL', known as equilibrium parameter. The next equation can determine the separation factor 'RL':

$$R_L = \frac{1}{1 + K_L C_0} \quad (20)$$

RL values [53] computed from the preceding equation are included in Table 1.

#### 2.2.5.2. Freundlich isotherm model

A German physical chemist presented an experimental isotherm for the non-ideal system in 1906 [49]. This model presumed that a multilayer adsorption process took place on a heterogeneous absorbent surface owing to the absence of homogeneous active sites. The heterogeneity factor ( $1/n$ ) that categorises Freundlich isotherm is not only limited to the creation of the monolayer but also for describing reversible adsorption systems. The following equalisation can represent this comparatively adequate practical isotherm:

$$q_e = K_F C_e \frac{1}{n} \quad (21)$$

where  $q_e$  is the adsorbed amount of MB at equilibrium (mg/g),  $C_e$  is the MB strength at equilibrium (mg/L),  $K_F$  is the

Table 1  
Type of isotherm based on RL values

RL value	Type of isotherm
RL > 1	Unfavourable
RL = 1	Linear
0 < RL < 1	Favourable
RL = 0	Irreversible

Freundlich constant ( $\text{dm}^3/\text{g}$ ), which is used as an indicator of the multilayer adsorptive capacity and adsorption effectiveness, whereas  $n$  is a heterogeneity factor (dimensionless) that represents adsorption intensity. Taking the logarithm of both sides gives the following linear form:

$$\ln q_e = \ln K_f + \frac{1}{n} \ln C_e \quad (22)$$

Therefore, values of  $K_f$  and  $1/n$  were investigated from the plot of  $\ln q_e$  vs.  $C_e$ .

#### 2.2.5.3. Temkin isotherm model

The Temkin isotherm anticipated the linear decrease in the heat of adsorption system in the adsorbent layer by covering the sorbent surface by dye molecules owing to the adsorbent-adsorbate interaction, and this drop is supposed to be linear rather than logarithmic. Additionally, this model assumed that the binding energies have a regular pattern, up to the highest binding energy. The nonlinear form of Temkin equation is presented below [52]:

$$q_e = \left( \frac{RT}{bT} \right) \ln KTC_e \quad (23)$$

where  $bT$  is the Temkin constant which is correlated to the heat of system ( $\text{J/mol}$ ) and  $KT$  is the Temkin constant that described the supreme confining energy of adsorbent and adsorbate ( $\text{L/g}$ ). Linearisation and arrangement of Eq. (22) results in

$$q_e = \left( \frac{RT}{bT} \right) \ln KT + \left( \frac{RT}{bT} \right) \ln C_e \quad (24)$$

By replacing constant  $RT/bT$  with the term  $B$  (constant), the linear equation becomes

$$q_e = B \ln KT + B \ln C_e \quad (25)$$

$bT$  and  $KT$  constants were evaluated from the straight line between  $q_e$  and  $C_e$ .

#### 2.2.5.4. D–R isotherm model

The D–R model is used for explaining the sorption isotherm of a single solute system. This isotherm is analogue to the Langmuir model, but it is more general as it does not refer to a homogeneous adsorbent surface or substantial adsorption potential. The nonlinear isotherm equation is stated by

$$q_e = q_{D-R} \exp(-K_{ad} \varepsilon^2) \quad (26)$$

where  $q_e$  is the total adsorbate molecule at equilibrium/gram of adsorbent ( $\text{mg/g}$ ).  $q_{D-R}$  is the D–R adsorption capacity ( $\text{mg/g}$ ),  $K_{ad}$  is the D–R constant ( $\text{mol}^2/\text{kJ}^2$ ) and interrelated to the adsorption energy.  $\varepsilon$  is Polanyi potential constant ( $\text{kJ/mol}$ ) [51]. Linearisation of Eq. (25) gives

$$\ln q_e = \ln q_{D-R} - K_{ad} \varepsilon^2 \quad (27)$$

$\varepsilon$  can be deliberate from the following equalisation:

$$\varepsilon = RT \ln \left( 1 + \frac{1}{C_e} \right) \quad (28)$$

where  $C_e$  is the MB concentration at equilibrium in the aqueous solution ( $\text{mg/L}$ ),  $R$  and  $T$  are the gas constant ( $\text{kJ/mol/K}$ ) and temperature in  $\text{K}$ , respectively.

Information about the physical and chemical characteristics of the adsorption process may be indicated by evaluating the mean free energy ( $E$ ) per molecule of MB adsorbed on the adsorbent surface. This energy can estimate via the D–R constant  $K_{ad}$  as follows:

$$E = \frac{1}{\sqrt{2K_{ad}}} \quad (29)$$

The style of the adsorption mechanism can be guesstimate by the magnitude of  $E$  ( $\text{kJ/mol}$ ) according to its value. For example, for  $20 > E > 8$ , the system was chemically controlled and for  $E < 8$  the process is physically monitored.

#### 2.2.6. Adsorption thermodynamics

The following equations can determine the thermodynamic parameters such as Gibbs free energy ( $\Delta G^\circ$ ), enthalpy ( $\Delta H^\circ$ ), and entropy ( $\Delta S^\circ$ ):

$$\ln K = -\frac{\Delta H^\circ}{RT} + \frac{\Delta S^\circ}{R} \quad (30)$$

$$\Delta G^\circ = \Delta H^\circ - T\Delta S^\circ \quad (31)$$

where  $K$  is the thermodynamic equilibrium constant of adsorption,  $\Delta S^\circ$  is the standard entropy change ( $\text{J/mol K}$ ), and  $\Delta H^\circ$  is the standard enthalpy change ( $\text{kJ/mol}$ ).  $\Delta G^\circ$  is the standard Gibbs free energy change ( $\text{kJ/mol}$ ) and  $T$  is system temperature ( $\text{K}$ ).  $R$  is the universal gas constant ( $8.314 \text{ J/mol K}$ ). However, the equilibrium adsorption constant ( $K$ ) can be investigated by [54]

$$K = \frac{\text{Dye concentration in the resin at equilibrium} \left( \frac{\text{mg}}{\text{g}} \right)}{\text{Dye concentration in solution at equilibrium} \left( \frac{\text{mg}}{\text{g}} \right)} \quad (32)$$

All thermodynamic parameters can be explored from the incline ( $\Delta H^\circ/R$ ) and intercept ( $\Delta S^\circ/R$ ) of the straight plot of  $\ln K$  against  $1/T$  [55].

### 3. Results and discussion

#### 3.1. Membrane characterisation

##### 3.1.1. Fourier transform infrared spectrophotometric analysis

Spectroscopic analysis plays a critical role in polymer characterisations. The use of such methods as Fourier

transform infrared spectrophotometry (FTIR) (Shimadzu FTIR-8400 S, Japan) is crucial in investigating the molecular structure of membranes. FTIR spectrums of PCA1.5 membranes are given in Fig. 2. It was explored that the particular band of  $-\text{COO}$  (ester bond) of CA appeared at  $1,741.87\text{ cm}^{-1}$ , while the characteristic absorption band for  $-\text{OH}$  group was noticed at  $3,479.70\text{ cm}^{-1}$ . Besides, the intensity of the peaks in the range of  $1,402.30\text{--}1,053.15\text{ cm}^{-1}$  was lower than that present in the original CA structure due to the reaction of the epoxy ring in ECH with the  $-\text{OH}$  located in CA as mentioned in our previous work [32]. Furthermore, the appearance of broadband at  $2,920.32\text{ cm}^{-1}$  was evidence for the introduction of the phosphoric group.

### 3.2. Effect of adsorption time and initial MB concentration

The consequence of the variation of the contact time on the MB removal percentage (%) and  $q$  (mg/g) of different MB concentrations is illustrated in Figs. 3 and 4. The results showed that the removal (%) increased by increasing the contact time. As well, the preliminary concentration is critical in controlling of reaching to the equilibrium state. The equilibrium time shifted to longer ones by increasing the initial MB concentration from 120 min of 10 ppm to 300 min of 100 ppm (Fig. 3). This observation indicated the surface adsorption system as the first stage and proved the necessity of the concentration gradient (driving force) to defeat the resistance to the MB transfer between the bulk and the solid phases [56]. Also, the establishment of the MB layer adsorbed

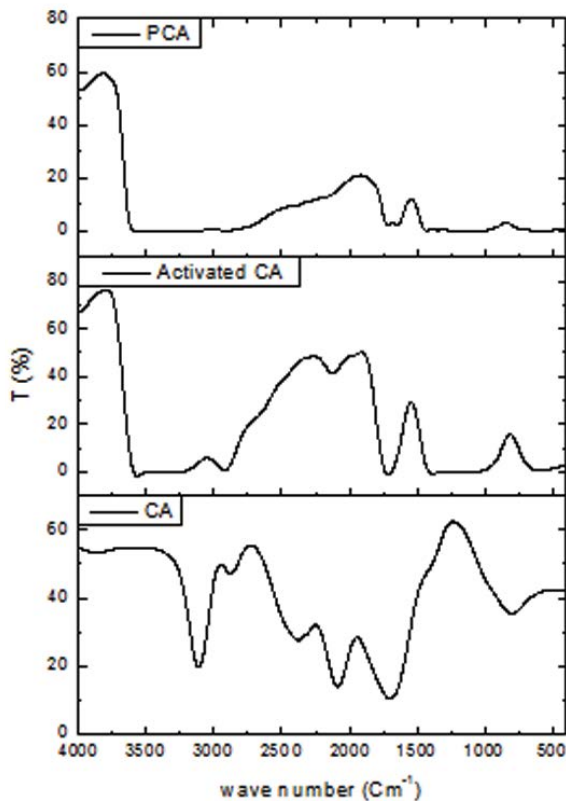


Fig. 2. FTIR spectra of pure CA, activated CA, and PCA1.5 membranes.

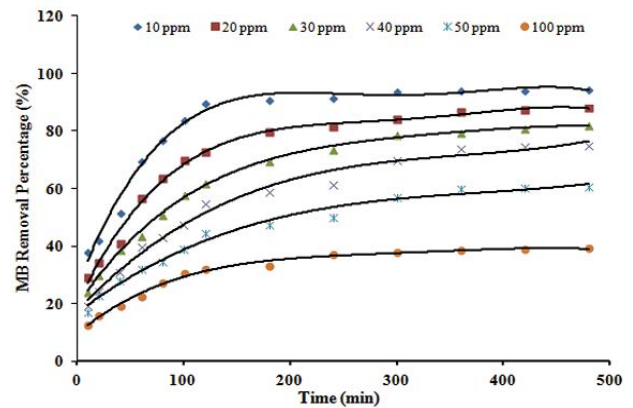


Fig. 3. Effect of adsorption time on the MB removal percentage (pH = 6, 0.2/50 mL, and at 298 K).

on the membrane surface at the early stage of the process reduces this force as a consequence of the reduction of the MB concentration between the liquid and the solid phases. The sorption capacity followed the same behaviour which increased almost linearly at the first 90 min of adsorption time, then started to decrease, and finally reached the equilibrium situation (Fig. 4). The impact of varying MB concentration on the removal (%) and  $q$  (mg/g) was carried out batch-wise using several initial MB concentrations at equilibrium time using 0.2 g/50 mL under constant pH (6) and temperature (298 K). This effect highly depends on the direct relationship among the MB level and the possible binding localities on a membrane surface [57]. It was manifest from Fig. 5 that the removal (%) decreased by increasing the original concentration from 10 to 100 ppm. This result is expected as at lower concentration, large surface area was available for MB cations, but as the concentration increased, the active sites become blocked and saturated. This trend may result from the electrostatic opposing forces amid the solid and bulk phases [58,59].

Alternatively, it was found that as the primary MB concentration increases, more molecules accumulate on the membrane surface. In addition, the extent of adsorbate

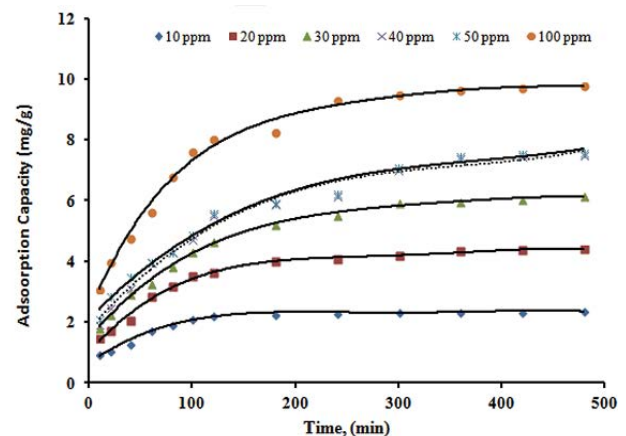


Fig. 4. Effect of adsorption time on the adsorption capacity for MB (pH = 6, 0.2/50 mL, and at 298 K).

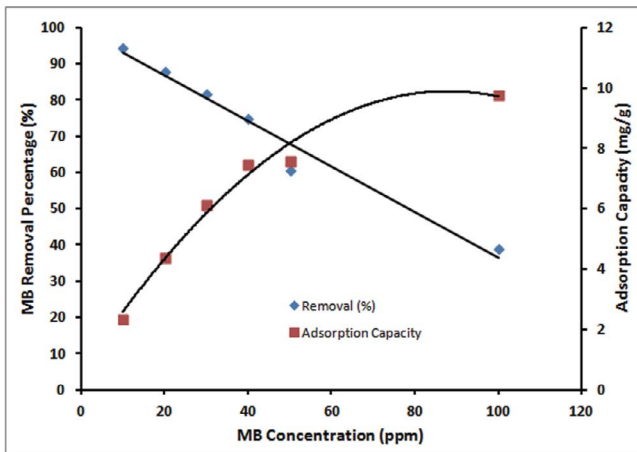


Fig. 5. Effect of initial dye concentration on the MB removal percentage and adsorption capacity at equilibrium (pH = 6, 0.2/50 mL, 480 min, and at 298 K).

molecules removed per gram PCA rises by growing the initial strength of MB with time, and the  $q$  (mg/g) varied from 2.3 to 9.7 mg/g as  $C_0$  ranged from 10 to 100 mg/L at equilibrium.

### 3.3. Effect of solution pH

Controlling the pH of the dye solution has a significant influence on the adsorption rate [61]. Because of its straight influence on the adsorptive capacity of the adsorbent surface towards the dye and the dissociative. The experiment was performed by using 0.2 g of PCA1.5 membrane/50 mL of 10 ppm dye solution, at 25°C for 2 h. Fig. 6 shows that the adsorption efficiency of MB increased considerably with the increase in pH values from 3 to 11. The maximum percent removal was 98.51% at pH 10 while increasing the pH above 10 has no significant effect. This investigation may be because the adsorption process depends on the affinity of the electrical charges on the adsorbent surface and progressively affected by the change in pH values [60]. Consequentially, the PCA1.5 surface has a net negative surface charge. In addition, increasing the pH enhances the negativity of the membrane surface; therefore, the surface charge density decreases and the electrostatic repulsions between the adsorbent and the

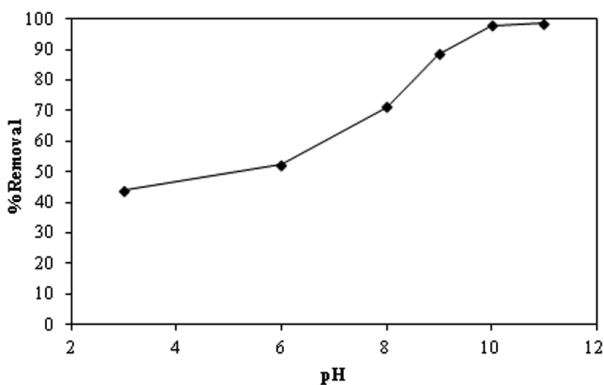


Fig. 6. The effect of the solution pH on the percent removal of MB from aqueous solution (0.2 g/50 mL of 10 ppm, 2 h, and 25°).

positively charged basic dyes are less, thereby increasing the extent of adsorption. Similar results have been reported elsewhere [61].

### 3.4. Adsorption kinetic models

The kinetic considerations of MB under different MB concentrations using the pseudo-1st-order (Fig. 7), the pseudo-2nd-order (Fig. 8), and Elovich (Fig. 9) models were calculated and summarized in Table 2. As shown from the tabulated data, the obtained correlation coefficient ( $R^2$ ) values are close to 1 in the following manner: the pseudo-2nd-order > Elovich > pseudo-1st-order models, respectively. Meanwhile, the calculated  $q_e$  anticipated from pseudo-2nd-order model agrees reasonably better with the experimental data. As a result, this model can accurately forecast the kinetics of MB adsorption on the PCA1.5 surface. Thus, the adsorption kinetics data were best described via the pseudo-2nd-order model. Also, chemisorption is considered the rate-limiting step of the adsorption system [62] relating strong forces through the sharing or exchanging of electrons between sorbent and sorbate.

In the same context, many publications refer that MB adsorption usually follows the pseudo-2nd-order kinetic

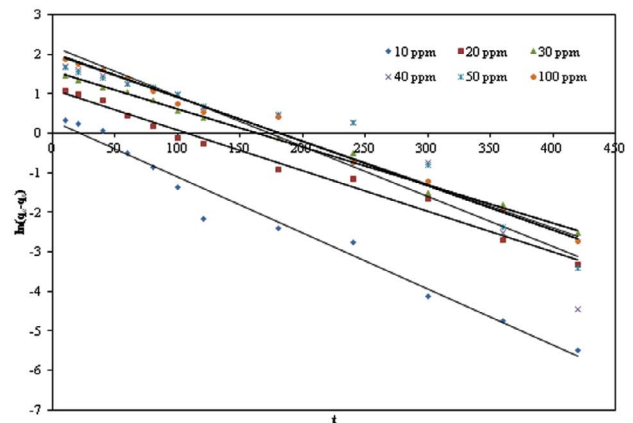


Fig. 7. Pseudo-first-order model for the adsorption of MB on PCA1.5 membranes.

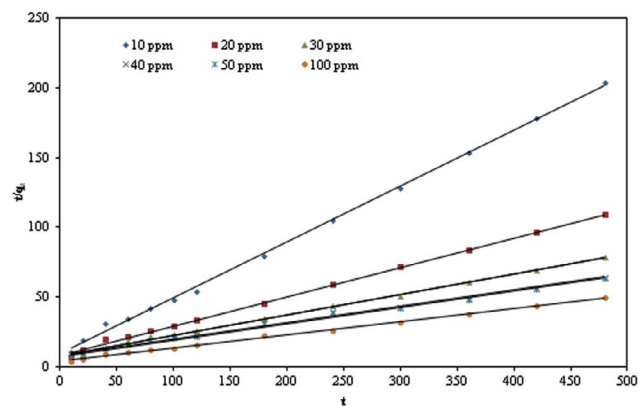


Fig. 8. Pseudo-second-order model for the adsorption of MB on PCA1.5 membranes.

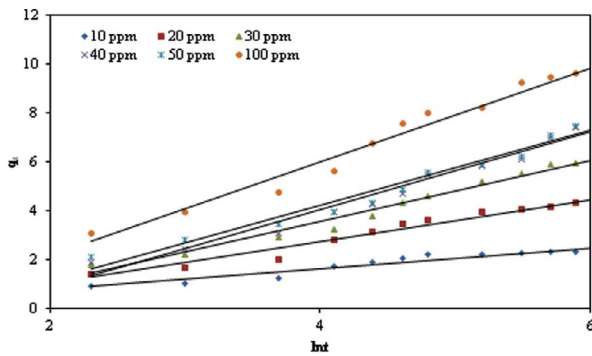


Fig. 9. Elovich model for the adsorption of MB on PCA1.5 membranes.

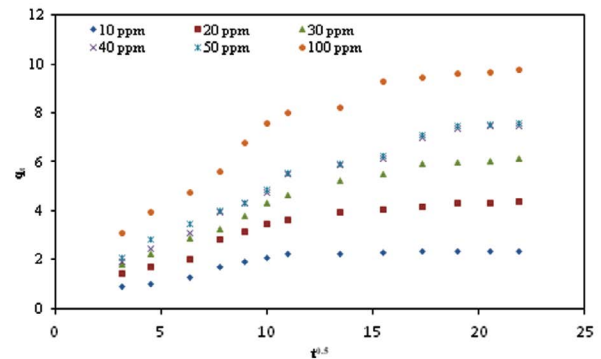


Fig. 10. The intraparticle diffusion model for the adsorption of MB on PCA1.5 membranes.

model [63–65]. In contrast, although the  $R^2$  values of the pseudo-1st-order dynamic shown in Table 2 are high enough at each MB concentration, the  $q_{e,cal}$  values deviate from the respective  $q_{e,exp}$  values. Thus, it is not appropriate to illustrate the MB adsorption by a PCA1.5 membrane, even if the correlation coefficient values are excellent.

### 3.5. Adsorption mechanism

#### 3.5.1. Intraparticle diffusion

As can be noticed from Fig. 10, the plot has a sharper portion in the beginning till 11 min which may express as quick adsorption step or outer surface adsorption and then

steady adsorption where the intraparticle distribution is the rate-limiting step. Finally, owing to the decrease in the adsorption concentration in bulk, the diffusion began to retard the equilibrium stage observed. A similar observation was obtained by other authors [66]. Plotting of  $q_t$  vs  $t^{0.5}$  results in straight lines did not pass by the origin, which suggests that despite the adsorption involves intraparticle diffusion but it is not the solely rate-determining step. Also, the positive intercept value ( $C$ ) gives evidence about the developed boundary layer and the character of the adsorption system. Furthermore, the anticipated values ( $C \neq 0$ ) as mentioned in Table 3 demonstrated the complexity of the adsorption method.

Table 2

Rate constants, correlation coefficients, experimental and calculated  $q_e$  values for the Pseudo-1st-, pseudo-2nd-order, and Elovich models at different initial MP concentrations

MB concentrations (mg/L)	$q_{e,exp}$	Pseudo-1st order				Pseudo-2nd order				Elovich model		
		$R^2$	$K_1$	$q_{e,cal}$	$\left(\frac{\Delta q}{q}\right)\%$	$R^2$	$q_{e,cal}$	$K_2$	$\left(\frac{\Delta q}{q}\right)\%$	$R^2$	$\beta$	$\alpha$
10	2.358	0.976	0.014	1.374	41	0.998	2.493	1.468	5	0.91	0.413	2.462
20	4.397	0.986	0.01	3.046	30	0.998	4.975	0.318	13	0.963	0.854	2.571
30	6.140	0.994	0.009	4.879	20	0.996	6.802	0.160	10	0.98	1.248	2.528
40	7.494	0.883	0.012	9.115	21	0.991	8.474	0.105	13	0.975	1.592	2.700
50	7.587	0.923	0.011	13.329	75	0.99	8.474	0.097	11	0.973	1.528	2.250
100	9.774	0.991	0.011	7.515	22	0.997	10.63	0.033	8	0.973	1.918	1.242

Table 3

Rate constants and correlation coefficients for the intraparticle diffusion, Dumwald-Wagner, and Boyd kinetic models at each initial MP concentration

MB concentration (ppm)	$q_{e,exp}$	Intraparticle diffusion model			Dumwald-Wagner model	Boyd model
		$R^2$	$K_p$	$C$	$R^2$	$R^2$
10	2.358	0.759	0.073	1.043	0.981	0.976
20	4.397	0.867	0.157	1.428	0.985	0.986
30	6.141	0.927	0.307	1.550	0.987	0.992
40	7.614	0.961	0.296	1.426	0.897	0.883
50	6.531	0.967	0.296	1.694	0.859	0.923
100	8.714	0.897	0.358	3	0.987	0.991

3.5.2. Boyd model

The linearity of the Boyd plots illustrated in Fig. 11 was significant in defining the definite step control. For instance, the particle diffusion mechanism controls the adsorption process when the plot is an uninterrupted line passed by the origin point. Otherwise, the process is governed by film diffusion mechanism [67]. For MB adsorption on the membrane surface, it was demonstrated that film diffusion controls the operation as the obtained line is straight but not crossing the origin especially at concentrations of MB higher than 10 ppm. Only for 10 ppm concentration, the line reached the (0, 0) point, which could be explained by the small depth of the patterned film diffusion layer as designated in Table 3.

3.5.3. D-W model

The empirical data were elaborated in Fig. 12 as a plot between  $\ln(1 - F^2)$  vs  $t$  for all MB initial concentrations.  $R^2$  values shown in Table 3 (0.981–0.987) illustrate the applicability of D-W kinetic model for the MB adsorption.

3.6. Adsorption isotherms

3.6.1. Langmuir and Freundlich

The linear fixture of the laboratory data for isotherm models was shown in Figs. 13 and 14, respectively. It was

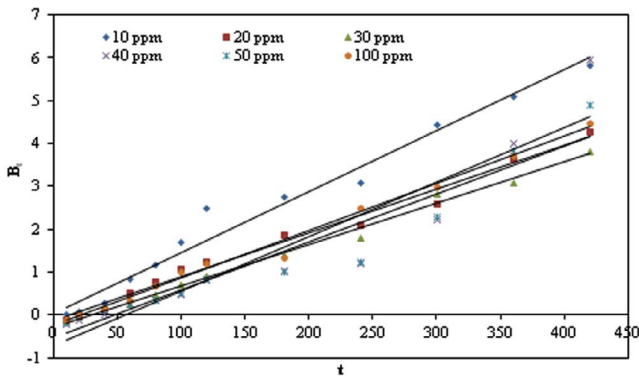


Fig. 11. Boyd model for the adsorption of MB on PCA1.5 membranes.

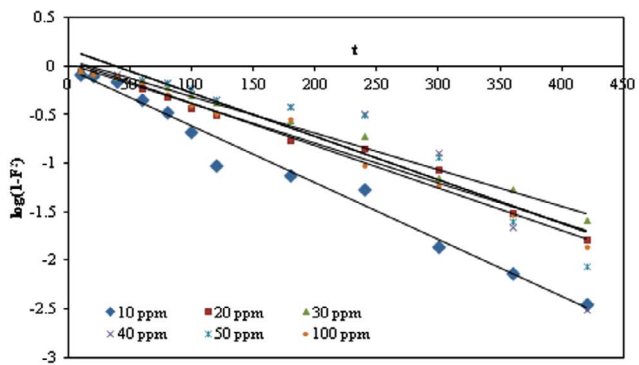


Fig. 12. D-W kinetic model for the adsorption of MB on PCA1.5 membranes.

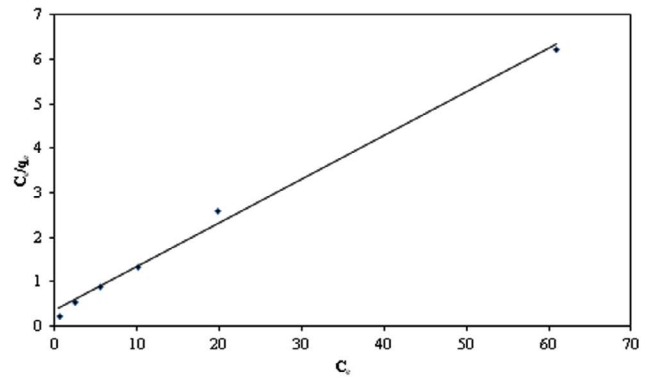


Fig. 13. Langmuir adsorption isotherm for MB adsorption using PCA1.5 adsorbents at numerous initial solution concentrations.

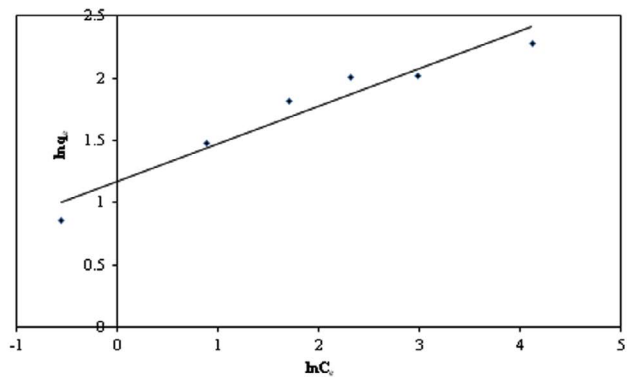


Fig. 14. Freundlich adsorption isotherm for MB adsorption using PCA1.5 adsorbents at numerous initial dye concentrations.

evident from Table 4 that the  $R^2$  value of Langmuir isotherm is very adjacent to 1 compared with that of Freundlich isotherm. Moreover, the estimated  $q_{max,exp}$  value by Langmuir model is about 10 mg/g [68,69], which indicates that prepared membranes are a comparable and suitable adsorbent for the elimination of MB from aqueous solution. According to the coefficient constants obtained from Langmuir model, RL values (0.747–0.228) for the adsorption of MB on the surface of PCA1.5 are less than 1 and greater than zero, demonstrating favourable adsorption process. Alternatively, the heterogeneity of dye adsorption was evaluated consistent with the heterogeneity factor ( $n$ ) value attained by the incline of the Freundlich isotherm model. It was observed that these values are much greater than 1, suggesting a nonlinear heterogeneous and favourable adsorption of dye molecules. This observation exhibited that the data are best fit to the Langmuir model than Freundlich isotherm.

3.6.2. Dubin-Radushkevich isotherm model

A design of  $\ln q_e$  vs  $\epsilon^2$  results in a continuous line of slope  $K_{ad}$  and an intercept of  $\ln q_{D-R}$  as shown in Fig. 15. It is noted from Table 4 that the  $R^2$  values are close to 1 indicating that the trial data obey D–R isotherm model [70,71]. Furthermore, the adsorption energy calculated from this model is less than 8, which implies that MB removal onto the membrane surface

Table 4

Langmuir, Freundlich, Dubin-Radushkevich, and Temkin adsorption isotherm parameters for MB sorption using PCA1.5 membrane

Isotherm model	Parameters		
Langmuir	$K_L$ (L/g) 29.577	$q_{max}$ (mg/g) 10.204	$R^2$ 0.994
Freundlich	$K_f$ (mg/g) 3.228	$n$ 3.322	$R^2$ 0.937
Dubin-Radushkevich	$K_{ad}$ (mol <sup>2</sup> /kJ <sup>2</sup> ) 0.186	$q_{D-R}$ (mg/g) $E$ (kJ/mol) 7.149 1.639	$R^2$ 0.811
Temkin	$KT$ (L/g) 1.02	$bT$ (J/mol) 0.0016	$R^2$ 0.982

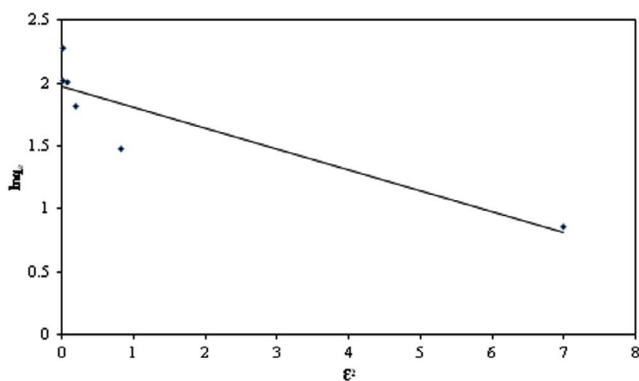


Fig. 15. Dubinin-Radushkevich adsorption isotherm for MB adsorption using PCA1.5 adsorbents at numerous initial dye concentrations.

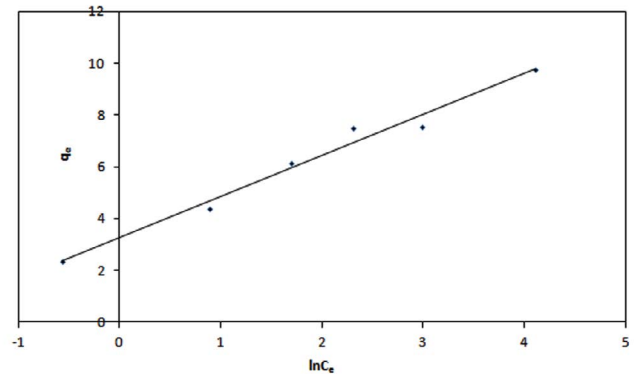


Fig. 16. Temkin adsorption isotherm for MB adsorption using PCA1.5 adsorbents at numerous initial dye concentrations.

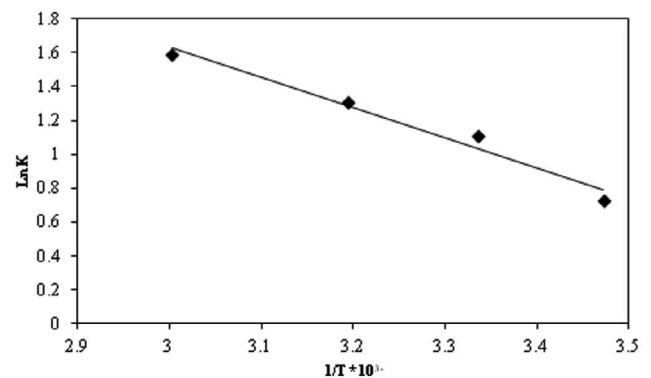
is a physical process, which illustrates the function of the electrostatic forces during adsorption mechanism.

### 3.6.3. Temkin isotherm model

As stated, the plot of the linear formula of Temkin equation is illustrated in Fig. 16. The Temkin parameters  $KT$  and  $bT$  are calculated and represented in Table 4. The calculation reported the highest binding energy expressed by  $KT$  as 1.002 L/g, while the heat of adsorption indicated by  $bT$  is nearly 0.0016 J/mol [72]. Also, this model signifies the identical configuration of the binding energy sites on the adsorbent surface [73] as the acquired  $R^2$  is approximately 1.

### 3.7. Thermodynamics

Fig. 17 and Table 5 exemplify the Van't Hoff plots of MB adsorption. The positive values of  $\Delta H^\circ$  suggest that the adsorption system is endothermic in nature and indicate that the apprehensive process reached equilibrium by consuming energy from the system, while the obtained negative  $\Delta G^\circ$  values indicate feasibility, involuntary, and favourable interaction of dye molecules towards the adsorbent [74]. However, the structural changes in the sorbent material [75]

Fig. 17.  $\ln K$  versus  $1/T$  according to Van't Hoff equation.

are approved by the positive  $\Delta S^\circ$  value and propose that the degree of randomness increased at the solid-liquid interface during the process [55].

### 3.8. Adsorption capacity

The adsorption potential of the processed PCA compared with that of other cellulosic matrices used for MB dye

Table 5  
Thermodynamic parameters

T (K)	$\Delta H^\circ$ (kJ/mol)	$\Delta S^\circ$ (J/mol K)	$\Delta G^\circ$ (kJ/mol)
288	14.715	57.699	-16.603
298			-17.180
313			-18.045
333			-19.199

Table 6  
Adsorption capacity of different cellulose matrices for MB dye

Cellulose matrices	Adsorption capacity (mg/g)	Reference
polyacrylic acid-grafted quaternized cellulose hydrogel	1,734.8	[75]
nanocrystalline cellulose	101	[76]
porous hemicellulose hydrogel	300–400	[77]
cellulose-graft-acrylic acid superabsorbent	2,197	[78]
Amidoximated PAN-g-cotton fabrics	13.6	[58]
Phosphonated cellulose acetate membranes	9.7	This work

adsorption process issues is tabulated in Table 6. From the table, it is quite clear that the obtained adsorption capability is moderately low in comparison with other published results [76]. This could be attributable to the relative hydrophobicity of the PCA membranes relative to the other matrices. In addition, the spongy nature is an important factor affecting sorption potential which directly has an impact on the superficial area available for adsorption process to take place.

#### 4. Conclusion

The study confirms that the adsorption process was efficient for MB amputation from industrial waste solutions. The results clearly demonstrated that PCA membranes contributed to adsorption mechanism through electrostatic interactions between phosphonic groups of the membrane and the cationic MB dye. The maximum dye removal (%) is concentration dependent as it decreases from 95% to 35% with increasing MB concentration from 10 to 100 ppm, whereas the adsorption potential ( $q$ ) increased to reach the maximum value (9.7 mg/g) at 100 ppm. In addition, the adsorption equilibrium behaviour of MB dye onto the PCA membranes followed the Langmuir adsorption isotherms ( $R^2 \sim 1$ ,  $q_{\max} = 10$  mg/g) suggesting a nonlinear heterogeneous and demonstrating favourable adsorption process in relation to calculated RL values. The sorption rate was established to conform pseudo-2nd-order model ideal with good correlation coefficients ( $R^2 \sim 1$ ) and 5% deviation error between  $q_{e,exp}$  and the  $q_{e,cal}$ .

Finally, the negative  $\Delta G^\circ$  values specified that dye adsorption onto sorbent membranes was viable and spontaneous. The positive  $\Delta H^\circ$  value depicted endothermic countryside of the adsorption progression.

#### References

- [1] Y. Esfandyari, Y. Mahdavi, M. Seyedsalehi, M. Hoseini, G.H. Safari, M.G. Ghozikali, H. Kamani, J. Jaafari, Degradation and biodegradability improvement of the olive mill wastewater by peroxi electrocoagulation/electrooxidation–electroflotation process with bipolar aluminum electrodes, *Environ. Sci. Pollut. Res.*, 22 (2014) 6288–6297.
- [2] J. Jafari, A. Mesdaghinia, R. Nabizadeh, M. Farrokhi, A.H. Mahvi, Investigation of anaerobic fluidized bed reactor/aerobic moving bed bio reactor (AFBR/MMBR) system for treatment of currant wastewater, *Iran. J. Public Health*, 42 (2013) 860–867.
- [3] J. Jaafari, A. Mesdaghinia, R. Nabizadeh, M. Hoseini, A.H. Mahvi, Influence of up flow velocity on performance and biofilm characteristics of anaerobic fluidized bed reactor (AFBR) in treating high-strength wastewater, *J. Environ. Health Sci. Eng.*, 12 (2014) 139.
- [4] Q. Liao, J. Sun, L. Gao, The adsorption of resorcinol from water using multi-walled carbon nanotubes, *Colloids Surf. A Physicochem. Eng. Asp.*, 312 (2008) 160–165.
- [5] B.H. Hameed, A.A. Ahmad, Batch adsorption of methylene blue from aqueous solution by garlic peel, an agricultural waste biomass, *J. Hazard. Mater.*, 164 (2009) 870–875.
- [6] P. Luo, Y.F. Zhao, B. Zhang, J.D. Liu, Y. Yang, J.F. Liu, Study on the adsorption of neutral red from aqueous solution onto hollow site nanotubes, *Water Res.*, 44 (2010) 1489–1497.
- [7] B. Yasemin, A. Haluk, A kinetics and thermodynamics study of methylene blue adsorption on wheat shells, *Desalination*, 194 (2006) 259–267.
- [8] K.R. Ramakrishna, T. Viraraghavan, Dye removal using low cost adsorbents, *Water Sci. Technol.*, 36 (1997) 189–196.
- [9] Y. Yan, M. Zhang, K. Gong, L. Su, Z. Guo, L. Mao, Adsorption of methylene blue dye onto carbon nanotubes: a route to an electrochemically functional nanostructure and its layer-by-layer assembled nanocomposite, *Chem. Mater.*, 17 (2005) 3457–3463.
- [10] V.J.P. Poots, G. Mckay, J.J. Healy, The removal of acid dye from effluent using natural adsorbents-II wood, *Water Res.*, 10 (1976) 1067–1070.
- [11] S.J. Allen, G. Mckay, J.F. Porter, Adsorption isotherm models for basic dye adsorption by peat in single and binary component systems, *J. Colloid Interface Sci.*, 280 (2004) 322–333.
- [12] V.K. Garg, M. Amita, R. Kumar, R. Gupta, Basic dye (methylene blue) removal from simulated wastewater by adsorption using India Rosewood sawdust: a timber industry waste, *Dyes Pigm.*, 63 (2004) 243–250.
- [13] S. Wang, Y. Boyjoo, A. Choueib, Z.H. Zhu, Removal of dyes from aqueous solution using fly ash and red mud, *Water Res.*, 39 (2005) 129–138.
- [14] M. Rafatullah, O. Sulaiman, R. Hashim, A. Ahmad, Adsorption of methylene blue on low-cost adsorbents: a review, *J. Hazard. Mater.*, 177 (2010) 70–80.
- [15] C.H. Ahn, Y. Baek, C. Lee, S.O. Kim, S. Kim, S. Lee, S.H. Kim, S.S. Bae, J. Park, J. Yoon, Carbon nanotube-based membranes: fabrication and application to desalination, *J. Ind. Eng. Chem.*, 18 (2012) 1551–1559.
- [16] W. Zhang, C. Zhou, W. Zhou, A. Lei, Q. Zhang, Q. Wan, Fast and considerable adsorption of methylene blue dye onto graphene oxide, *Bull. Contam. Toxicol.*, 87 (2011) 86–90.
- [17] S.R. Popuri, Y. Vijaya, V.M. Boddu, A. Krishnaiah, Adsorptive removal of copper and nickel ions from water using chitosan coated PVC beads, *Bioresour. Technol.*, 100 (2009) 194–199.
- [18] Z.H. Hu, A.M. Omer, X.K. OuYang, D. Yu, Fabrication of carboxylated cellulose nanocrystal/sodium alginate hydrogel beads for adsorption of Pb(II) from aqueous solution, *Int. J. Biol. Macromol.*, 108 (2018) 149–157.

- [19] X.K. Ou-Yang, L.Y. Yang, A.M. Omer, Fabrication of a magnetic cellulose nanocrystal/metal–organic framework composite for removal of Pb(II) from water, *ACS Sustain. Chem. Eng.*, 5 (2017) 10447–10458.
- [20] M. Zafar, M. Ali, S.M. Khan, T. Jamil, M.T.Z. Butt, Influence of glycol additives on the structure and performance of cellulose acetate/zinc oxide blend membranes, *Desalination*, 270 (2011) 98–104.
- [21] D. Emadzadeh, W.J. Lau, T. Matsuura, M. Rahbari-Sisakht, A.F. Ismail, A novel thin film composite forward osmosis membrane prepared from PSf-TiO<sub>2</sub> nanocomposite substrate for water desalination, *Chem. Eng. J.*, 237 (2014) 70–80.
- [22] J. Bujdak, P. Komadel, Interaction of methylene blue with reduced charge montmorillonite, *J. Phys. Chem. B.*, 101 (1997) 9065–9068.
- [23] G. Chen, J. Pan, B. Han, H. Yan, Adsorption of methylene blue on montmorillonite, *J. Dispers. Sci. Technol.*, 20 (1999) 1179–1187.
- [24] J.S. Taurozzia, H. Arul, V.Z. Bosak, A.F. Burban, T.C. Voice, M.L. Bruening, V.V. Tarabara, Effect of filler incorporation route on the properties of polysulfone-silver nanocomposite membranes of different porosities, *J. Membr. Sci.*, 325 (2008) 58–68.
- [25] S.M. Hosseini, S.S. Madaeni, A.R. Khodabakhshi, Preparation and characterization of heterogeneous cation exchange membranes based on s-poly vinyl chloride and polycarbonate, *Sep. Sci. Technol.*, 46 (2011) 794–808.
- [26] S.M. Hosseini, S.S. Madaeni, A.R. Khodabakhshi, Preparation and characterization of ABS/HIPS heterogeneous cation exchange membranes with various blend ratios of polymer binder, *J. Membr. Sci.*, 351 (2010) 178–188.
- [27] A.R. Khodabakhshi, S.S. Madaeni, S.M. Hosseini, Effect of polymers blend ratio binder on electrochemical and morphological properties of PC/S-PVC-based heterogeneous cation-exchange membranes, *J. Appl. Polym. Sci.*, 120 (2011) 644–656.
- [28] B.R. Locke, M. Sato, P. Sunka, M.R. Hoffmann, J.S. Chang, Electrohydraulic discharge and nonthermal plasma for water treatment, *Ind. Eng. Chem. Res.*, 45 (2006) 882–905.
- [29] R.K. Nagarale, G.S. Gohil, V.K. Shahi, R. Rangarajan, Preparation and electrochemical characterization of cation-exchange membranes with different functional groups, *Colloids Surf., A*, 251 (2004) 133–140.
- [30] R.K. Nagarale, V.K. Shahi, S.K. Thampy, R. Rangarajan, Studies on electrochemical characterization of polycarbonate and polysulfone based heterogeneous cation-exchange membranes, *React. Funct. Polym.*, 61 (2004) 131–138.
- [31] P.V. Vyas, B.G. Shah, G.S. Trivedi, P. Ray, S.K. Adhikary, R. Rangarajan, Characterization of heterogeneous anion-exchange membrane, *J. Membr. Sci.*, 187 (2001) 39–46.
- [32] M.S. Mohy Eldin, M.H. Abd Elmageed, A.M. Omer, T.M. Tamer, M.E. Yossuf, R.E. Khalifa, Development of novel phosphorylated cellulose acetate polyelectrolyte membranes for direct methanol fuel cell application, *Int. J. Electrochem. Sci.*, 11 (2016) 3467–3491.
- [33] H.C. Chiu, J.J. Huang, C.H. Liu, S.Y. Suen, Batch adsorption performance of methyl methacrylate/styrene copolymer membranes, *React. Funct. Polym.*, 66 (2006) 1515–1524.
- [34] R.L. Liu, Y. Liu, X.Y. Zhou, Z.Q. Zhang, J. Zhang, F.Q. Dang, Biomass-derived highly porous functional carbon fabricated by using a free-standing template for efficient removal of methylene blue, *Bioresour. Technol.*, 154 (2014) 138–147.
- [35] B.S. Inbaraj, C.P. Chiu, G.H. Ho, J. Yang, B.H. Chen, Removal of cationic dyes from aqueous solution using an anionic poly-gamma-glutamic acid-based adsorbent, *J. Hazard. Mater. B.*, 137 (2006) 226–234.
- [36] K.G. Bhattacharyya, A. Sharma, Adsorption of Pb(II) from aqueous solution by *Azadirachta indica* (Neem) leaf powder, *J. Hazard. Mater.*, 113 (2004) 97–109.
- [37] A.K. Jain, V.K. Gupta, A. Bhatnagar, Suhas, Utilization of industrial waste products as adsorbents for the removal of dyes, *J. Hazard. Mater. B*, 101 (2003) 31–42.
- [38] G. McKay, The adsorption of basic dye onto silica from aqueous-solution solid diffusion- model, *Chem. Eng. Sci.*, 39 (1984) 129–138.
- [39] S. Lagergren, About the theory of so-called adsorption of soluble substances, *K. Sven. Vetensk. Akad. Handl.*, 24 (1898) 1–39.
- [40] Y.S. Ho, G. McKay, Pseudo-second order model for sorption process, *Biochemistry*, 34 (1999) 451–465.
- [41] Y. Sağ, Y. Aktay, Kinetic studies on sorption of Cr(VI) and Cu(II) ions by chitin, chitosan and *Rhizopus arrhizus*, *Biochem. Eng. J.*, 12 (2002) 143–153.
- [42] C. Aharoni, F.C. Tompkins, Kinetics of adsorption and desorption and the Elvoich equation, *Adv. Catal.*, 21 (1970) 1–49.
- [43] M. Özacar, Equilibrium and kinetic modeling of adsorption of phosphorus on calcined alunite, *Adsorption*, 9 (2003) 125–132.
- [44] Y. Önal, C. Akmil-Başar, D. Eren, Ç. Sarıcı-Özdemir, T. Depci, Adsorption kinetics of malachite green onto activated carbon prepared from Tunçbilek lignite, *J. Hazard. Mater.*, 128 (2006) 150–157.
- [45] H. Wang, C. Jindong, Z. Zhai, C. Jindong, Study on thermodynamics and kinetics of adsorption of p-toluidine from aqueous solution by hypercrosslinked polymeric adsorbents, *Environ. Chem.*, 23 (2004) 192–196.
- [46] G.E. Boyd, W. Adamson, L.S. Myers, The exchange adsorption of ions from aqueous solutions by organic zeolites; kinetics, *J. Am. Chem. Soc.*, 69 (1947) 2836–2848.
- [47] R. Bhattacharyya, S.K. Ray, Kinetic and equilibrium modeling for adsorption of textile dyes in aqueous solutions by carboxymethyl cellulose/poly (acrylamide-cohydroxyethyl methacrylate) semi interpenetrating network hydrogel, *Polym. Eng. Sci.*, 53 (2013) 2439–2453.
- [48] I. Langmuir, The constitution and fundamental properties of solids and liquids. Part I. Solids, *J. Am. Chem. Soc.*, 38 (1916) 2221–2295.
- [49] H.M.F. Freundlich, Über Die Adsorption in Lösungen, *Zeitschrift für Physikalische Chemie*, Leipzig, *J. Phys. Chem.*, 57A (1906) 385–470.
- [50] M. Belhachemi, F. Addoun, Comparative adsorption isotherms and modeling of methylene blue onto activated carbons, *Appl. Water Sci.*, 1 (2011) 111–117.
- [51] M.M. Dubinin, L.V. Radushkevich, E.D. Zaverina, Sorption and structure of active carbons, *J. Phys. Chem.*, 2 (1947) 1351–1362.
- [52] M.J. Temkin, V. Pyzhev, Kinetics of ammonia synthesis on promoted iron catalysts, *J. Phys. Chem.*, 13 (1939) 851–867.
- [53] K.R. Hall, L.C. Eagleton, A. Acrivos, T. Vermeulen, Pore- and solid-diffusion kinetics in fixed-bed adsorption under constant-pattern conditions, *Ind. Eng. Chem. Fundam.*, 5 (1966) 212–223.
- [54] Y. Yu, Y. Zhuang, Z.H. Wang, Adsorption of water soluble dye onto functionalized resin, *J. Colloid Interface Sci.*, 242 (2001) 288–293.
- [55] S.M. Al-Rashed, A.A. Al-Gaid, Kinetic and thermodynamic studies on the adsorption behavior of Rhodamine B dye on Duolite C-20 resin, *J. Saudi Chem. Soc.*, 16 (2012) 209–215.
- [56] H. Ouasif, S. Yousfi, M.L. Bouamrani, M. El Kouali, S. Benmokhtar, M. Talbi, Removal of a cationic dye from wastewater by adsorption onto natural adsorbents, *J. Mater. Environ. Sci.*, 4 (2013) 1–10.
- [57] S.A. Umoren, U.J. Etim, A.U. Israel, Adsorption of methylene blue from industrial effluent using poly (vinyl alcohol), *J. Mater. Environ. Sci.*, 4 (2013) 75–86.
- [58] M.S. Mohy Eldin, M.H. Gouda, M.A. Abu-Saied, Yehia M.S. El-Shazly, H.A. Farag, Development of grafted cotton fabrics ions exchanger for dye removal applications: methylene blue model, *Desal. Wat. Treat.*, 57 (2016) 22049–22060.
- [59] N. Barka, S. Qouzal, A. Assabbane, A. Nounhan, Y.A. Ichou, Removal of reactive yellow 84 from aqueous solutions by adsorption onto hydroxyapaite, *J. Saudi Chem. Soc.*, 15 (2011) 263–267.
- [60] S. Banerjee, M.C. Chattopadhyaya, V. Srivastava, Y.C. Sharma, Adsorption studies of methylene blue onto activated saw dust: kinetics, equilibrium, and thermodynamic studies, *Environ. Prog. Sustain. Energy*, 33 (2014) 790–799.
- [61] S. Saber-Samandari, H.O. Gulcan, S. Saber-Samandari, M. Gazi, Efficient removal of anionic and cationic dyes from an aqueous

- solution using pullulan-graft-polyacrylamide porous hydrogel. *Water Air Soil Poll.*, 225 (2014) 2177–2191.
- [62] J. Kalmar, G. Lente, I. Fabian, Kinetics and mechanism of the adsorption of methylene blue from aqueous solution on the surface of a quartz cuvette by on-line UV-Vis spectrophotometry, *Dyes Pigm.*, 127 (2016) 170–178.
- [63] C. Liu, A.M. Omer, X.k. Ouyang, Fabrication of ofloxacin imprinted polymer on the surface of magnetic carboxylated cellulose nanocrystals for highly selective adsorption of fluoroquinolones from water, *Int. J. Biol. Macromol.*, 107 (2018) 453–462.
- [64] M.S. Mohy Eldin, K.M. Aly, Z.A. Khan, A.E.M. Mekky, T.S. Saleh, A.S. Al-Bogami, Removal of methylene blue from synthetic aqueous solutions with novel phosphoric acid-doped pyrazole-g-poly(glycidyl methacrylate) particles: kinetic and equilibrium studies, *Desal. Wat. Treat.*, 57 (2016) 27243–27258.
- [65] T.M. Elmorsi, Equilibrium isotherms and kinetic studies of removal of methylene blue dye by adsorption onto miswak leaves as a natural adsorbent, *J. Environ. Prot.*, 2 (2011) 817–827.
- [66] A.S. Özcan, A. Özcan, Adsorption of acid dyes from aqueous solutions onto acid-activated bentonite, *J. Colloid Interface Sci.*, 276 (2004) 39–46.
- [67] R. Djeribi, O. Hamdaoui, Sorption of copper (II) from aqueous solutions by cedar sawdust and crushed brick, *Desalination*, 225 (2008) 95–112.
- [68] D. Mohan, K.P. Singh, Single- and multi-component adsorption of cadmium and zinc using activated carbon derived from bagasse-an agricultural waste, *Water Res.*, 36 (2002) 2304–2318.
- [69] N.K. Lazaridis, G.Z. Kyzas, A.A. Vassiliou, D.N. Bikiaris, Chitosan derivatives as biosorbents for basic dyes, *Langmuir*, 23 (2007) 7634–7643.
- [70] J.j. Gao, Y. Qin, T. Zhou, D.D. Cao, P. Xu, D. Hochstetter, Y.F. Wang, Adsorption of methylene blue onto activated carbon produced from tea (*Camellia sinensis* L.) seed shells: kinetics, equilibrium, and thermodynamics studies, *J. Zhejiang Univ. Sci. B*, 14 (2013) 650–658.
- [71] D. Balarak, J. Jaafari, Gh. Hassani, Y. Mahdavi, I. Tyagi, S.h. Agarwal, V.K. Gupta, The use of low-cost adsorbent (Canola residues) for the adsorption of methylene blue from aqueous solution: isotherm, kinetic and thermodynamic studies. *Colloids Interf. Sci. Commun.*, 7 (2015) 16–19.
- [72] M. Polanyi, Theories of the adsorption of gases. A general survey and some additional remarks, *Trans. Faraday Soc.*, 28 (1932) 316–332.
- [73] M. Makeswari, T. Santhi, M.R. Ezhilarasi, Adsorption of methylene blue dye by citric acid modified leaves of *Ricinus communis* from aqueous solutions, *J. Chem. Pharm. Res.*, 8 (2016) 452–462.
- [74] I. Tan, B.H. Hameed, A.L. Ahmad, Adsorption of basic dye (methylene blue) onto activated carbon prepared from rattan sawdust, *Chem. Eng. J.*, 127 (2007) 111–119.
- [75] K.G. Bhattacharyya, A. Sharma, Kinetics and thermodynamics of methylene blue adsorption on neem (*Azadirachta indica*) leaf powder, *Dyes Pigm.*, 65 (2005) 51–59.
- [76] D. Ghosh, K.G. Bhattacharyya, Adsorption of methylene blue on kaolinite, *Appl. Clay Sci.*, 20 (2002) 295–300.
- [77] X.-F. Sun, Z. Gan, Z. Jing, H. Wang, D. Wang, Y. Jin, Adsorption of methylene blue on hemicellulose-based stimuli-responsive porous hydrogel, *J. Appl. Polym. Sci.*, 132 (2015) 41606–41615.
- [78] Y. Zhou, S. Fu, H. Liu, S. Yang, H. Zhan, Removal of methylene blue dyes from wastewater using cellulose-based superadsorbent hydrogels, *Polym. Eng. Sci.*, 51 (2011) 2417–2424.